Germanium monolayer doping: successes and challenges for the next generation Ge devices

Francesco Sgarbossa [a,b,*]

[a] *Università degli Studi di Padova, Dipartimento di Fisica e Astronomia, via Marzolo 8, 35131, Padova, Italy*
[b] *Istituto Nazionale di Fisica Nucleare, Laboratori Nazionali di Legnaro, viale dell'Università 2, 35020, Legnaro, PD, Italy*

ARTICLE INFO

ABSTRACT

The growing interest in nanoelectronics and photonics, combined with the development of new germanium-based devices, provide the impetus to develop new doping methods suitable to new germanium challenges. The monolayer doping technique is one of the most promising techniques for nanostructure doping, especially for the possibility to perform conformal doping on nanostructured materials, the complete absence of lattice damage, the high control of the dopant and the reduction of the stochastic doping effects. In this paper, works that develop the monolayer doping technique on germanium will be described and analyzed, highlighting advantages and disadvantages of different possible approaches to Ge doping and finally outlining the future steps for the implementation of monolayer doping technique on device manufacturing.

1. Introduction

The study of new doping techniques in semiconductor field is arising from the continuous demand for high performance devices. During the last few decades, the main results in microelectronics have been obtained by the *device scaling* that allowed a continuous increasing of device performance by reducing the size of each transistor [1]. This historical progress was well described by the empirical Moore's Law. Nowadays, it's clear that new approaches to the problem are required since the microelectronics industries have already reached few nanometer devices presenting complex 3D shaping [2]. The traditional silicon planar architectures are now being slowly replaced by non-planar devices (e.g. multigate FETs), that minimizing some of the most important planar geometry issues, such as the high leakage current increase, which derives from the device scaling [1], and allows a better device switching control with lower power consumption thanks to the multi-gate geometry. Unfortunately, the current industrial process lines are based on standard industrial doping methods that were developed for planar geometry: adapting these methods for doping 3D nanostructured devices remains a challenging task [3]. As a matter of fact, the ion implantation doping technique presents several issues, such as stochastic doping issue at the nanoscale (i.e. large doping variability in small doped volume), it is not intrinsically conformal doping technique and it induce a lattice damage into the implanted material that must be restored [3].

On the other hand, the utilization of various semiconductor materials has been explored, with a focus on high mobility materials that are compatible with existing industrial silicon technology. One of the most interesting materials is germanium, which has very high mobility values for both carriers (holes 1900 $cm^2V^{-1}s^{-1}$ and electrons 3900 $cm^2V^{-1}s^{-1}$ at room temperature [4]) and offers excellent compatibility with silicon substrates, thanks to extensive research dedicated to the growth of germanium on silicon. Moreover, new researches disclose the possibility to use this material also for photonics [5–7], photovoltaics [8], plasmonic gas sensing [5], nano-electronics [4] and radiation detection [9, 10] in addition to other classical applications, for-instance IR detector [11], photodetectors [12], microwaves devices [13] and high performance devices [14] using Ge_xSi_{1-x} alloys. Beyond nanoelectronics, the possibility to use Ge as an optical active material arising from the possibility to induce a direct gap transition as a consequence of a band structure modification by high n-type doping [15] and/or high strain [16,17]. Germanium has now become one of the most promising materials for quantum computing device manufacturing: germanium holes spin quantum dots are used for the creation of qubit quantum processor, and the successfully creation of 4 qubits processor has disclosed the possibility to interconnect a larger number of qubits, which is now one of the most challenging tasks in this research field [18,19]. Thanks to these reasons, germanium is experiencing a new golden period in

---

* Università degli Studi di Padova, Dipartimento di Fisica e Astronomia, via Marzolo 8, 35131, Padova, Italy.
  E-mail address: francesco.sgarbossa@unipd.it.

semiconductor research, and several works has been published in germanium related fields. Indeed, the last 2020 IRDS Semiconductor Roadmap pointed out that Ge and SiGe materials are gaining importance as high mobility channels materials [20].

An interesting doping method that can meet these requirements of most the above applications is monolayer doping technique (MLD). Pioneered by the group of prof. Javey [21] on silicon, MLD is an ex situ non-destructive doping technique that consists of a controlled deposition of a precursor at the surface of a semiconductor that, after a proper thermal annealing is able to release and diffuse a dopant specie in the underlying target material. The precursor is a molecule that is chemisorbed or physisorbed at the surface of a material by chemical or physical deposition method. The most common route is a wet chemical deposition in which the molecule is adsorbed on the surface because of a thermally induced deposition procedure. Thanks to the use of self-limiting adsorption processes, the deposited dose is well controlled and the nature of these adsorptions normally guaranteed a surface conformal behavior. After the adsorption, the monolayer must be properly treated to promote the molecular fragmentation, fostering the release and diffusion of atomic species. Rapid and conventional thermal treatments are commonly employed to fragment molecules and promote dopant in-diffusion: however, alternative out-equilibrium techniques have also been studied as alternatives to standard processes. Nowadays, various variants of monolayer doping technique have been developed [22]: *Monolayer Contact Doping* (MLCD), *Remote Monolayer Doping* (r-MLD) and the *Gas Phase Monolayer Doping* (GP-MLD) are the most used variants of the methodology. According to the MLCD and r-MLD procedures, the monolayer is formed on a different surface from the one to be doped. MLCD exploits the contact between the target material and the functionalized surface to dope a different material than the monolayer functionalized one [23], while the r-MLD use a mask as a spacer between the source and the target material, preventing the direct contact [24]. Thanks to these methodologies, it is possible to separate the chemical adsorption process and the doped target, thus alleviating some constrains that can arise by the doped target surface and preventing a possible use of a capping layer. On the other hand, GP-MLD is based on the formation of a self-limiting monolayer from a gas phase deposition, avoiding the standard MLD wet chemical approach for the molecular adsorption and exploiting the possibility of fluxing a molecular precursor into an inert or vacuum chamber.

A potential limitation of the monolayer doping technique is the challenge of precisely tuning the dopant surface density. This difficulty arises because the deposited dopant's areal concentration is inherently linked to the self-limiting behavior of the adsorbate's interaction with the surface. The number of adsorbed molecules is typically determined by either the saturation of substrate functional groups or the reduction of surface-molecule interactions, which dictates the number of layers that can be physisorbed. As initially tested by Javey group [21] and later explored further by Ye and co-workers [25], the number of adsorbed molecules can be tuned by a *Mixed-Monolayer Doping Approach*, which involves the use of similar molecules during the monolayer deposition. In this approach, a certain fraction of the molecules contains the dopant atom (as an example, B atoms), while the remaining fraction lacks dopant species. By employing this technique, the authors demonstrate the possibility to fine-tune the silicon substrate doping, namely showing that the sample's resistance is correlated with the molecule surface density that contains dopant species. Thanks to this experiment, a further parameter can be controlled during MLD, making this technique more flexible, thus greatly enhanced the potential use of MLD with nanostructures. The same effect can be obtained also by tuning the molecular precursor footprint: as the steric size of the molecule increases, it corresponds to a progressively smaller number of doping atoms adsorbed on the surface, thus allowing the surface density of dopant to be changed. These approaches have the potential to be extended to other substrates and others chemisorption processes, making this study the forerunner for other adsorption mechanisms.
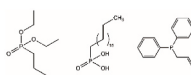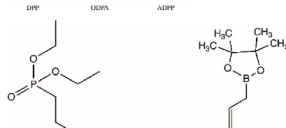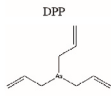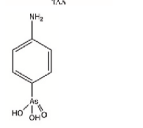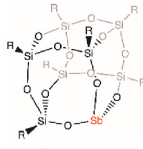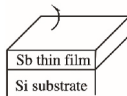
Monolayer doping was initially tested on silicon substrates [21,23, 25–33] and on silicon dioxide surfaces [28,34–36], but nowadays it has been applied to a large number of material, such as germanium [37–40] (see Table 1) silicon germanium alloys [41], III-V semiconductors [42]. The slow adoption of this technique from silicon to other materials could be related to the different behavior exhibited by each material surface and in some particular cases, on the lack of in-depth studies of surface reactivity and molecular adsorption. For an example, silicon and germanium show a completely different surface behavior, such as a different surface oxidation, a different ambient stability and many others. Whilst significant research has been conducted on surface chemistry reactions on germanium [43,44], there is still a need for comprehensive studies on adsorption behavior, molecule stability, and diffusion from monolayer sources.

The germanium tendency to oxidize, its poor stability to chemical passivation, the presence of more than one oxide are some of the main reasons why silicon chemistry cannot be easily applied also on germanium. Moreover, Ge has a lower melting point than Si (938 °C compared to 1414 °C) and completely different dopant diffusion coefficients, placing a new limit to the thermal budget for the thermal molecular fragmentation and new needs for dopant diffusion and activation processes.

2. Germanium surface treatments for oxide removal and surface functionalization

The first step of the monolayer doping technique involves preparing the substrate surface. This preparation entails removing residual organic, metal, and dust contaminants from the surface. In addition, the surface must be prepared to facilitate molecular adsorption through either chemisorption or self-limited physisorption. In many instances,

Table 1
Summary of the main characteristics of analyzed literature works.

Dopant atom(s)	MLD typology	Precursor(s)	Work(s)
P	*Wet – mesitylene reflux*	DPP ODPA ADPP	[37, 39]
P, B	*Gas phase deposition*	DPP ABAPE	[80]
As	*Wet – isopropanol or mesitylene UV light*	TAA	[40, 81]
As	*Wet – T bag method*	Arsanilic acid	[82]
Sb	*Wet – acetonitrile reflux*		[83]
Sb	*Gas phase deposition*	Sb₄ gas Sb thin film / Si substrate	[53]

meeting these surface requirements necessitates the removal of native oxide from germanium and the establishment of surface chemical functionalization.

Germanium naturally exhibits two different oxides: the water-insoluble GeO (where Ge has a formal oxidation number +2) and the water soluble GeO_2 (where Ge has a formal oxidation number +4). GeO_x native oxide is formed within a few minutes air exposure [45], varying depending on the starting surface termination [46], while the formed oxide composition is unstable over time. The most abundant native oxide component is GeO_2, but GeO and suboxide components are always present, especially during the first oxidation steps [47]. This behavior is shown in the most studied crystallographic faces, Ge (100) and (111), with no significant differences. This makes both Ge surface treatments and surface passivation extremely challenging as compared to the silicon case [48]. Moreover, the germanium native oxide presents a poor interface with Ge, presenting sub-oxide layers, which results in a high-density electronic defective layer, preventing the use of germanium oxide as a high-*k* material [49]. Indeed, extensive research has been conducted in recent years to identify the most effective procedures for cleaning the germanium surface. This process is crucial not only for achieving successful high-k integration to ensure reliable low-density trap interfaces but also for the initial monolayer doping task, which requires surface preparation before molecular adsorption can take place.

The germanium oxide is unstable above 390 °C [50] since the reaction $Ge_{(s)} + GeO_{2\ (s)} -> GeO_{(g)}$ take place, which means that a thermal oxide desorption process is thermally activated at the surface of germanium [51,52]. As a matter of fact, germanium oxide cannot be easily grown by using a controlled high temperature thermal treatment as in the silicon case, since germanium oxide starts to desorb from the surface as $GeO_{(g)}$ and it disappears from the surface of germanium [44]. On the other hand, this peculiar behavior can be used as a surface cleaning procedure, especially when combined with other high temperature Ge processing, as reported in the literature [53].

The most commonly used strategies for germanium oxide growing are wet oxidation processes using H_2O_2, HNO_3 and H_2O at different concentrations: probably the most used oxidant is a 30% solution of H_2O_2 [54,55] which prevalently form GeO_x with a very low amount of GeO_2. This can be related to its high solubility in water that dissolve the GeO_2 component in the oxidant solution, leaving the GeO_x suboxide component on the surface. The wet chemical oxidation is widely used as a previous step for oxide removal procedures or is used alternating oxidation and acid attack for a better surface contaminant removal procedure [44]. Other methods and mechanism studies are present in the literature [56–59], but they will not be treated here.

There are several different typologies of GeO_x removal procedures [60] that can be categorized in: UV/ozone, oxygen plasma, ion sputtering and Ge regrowth, and wet chemical treatments. Although some of the previous treatments are effective for the oxide removal, the wet chemical approaches better meet the MLD requirements, such as the need for a specific surface termination to create active sites for monolayer chemisorption and a higher compatibility with molecular adsorption, which are a wet chemical approach too. The most used wet oxide removal processes are based on warm water and a subsequent surface acid treatment. The warm water normally removed the most of GeO_2 component [54], while the acid dissolve most of the sub-oxide GeO_x components. Hydrofluoridric acid is one of the most used acid for the GeO_x removal and leads to a Ge-H_x surface termination (Fig. 1) [61] without consuming Ge substrate. Several works try to optimize this process, in order to maximize the surface –H termination coverage and to minimize the surface roughness as a consequence of the acid attack [62]. A water solution with 10% of HF for a few minutes (5–10 min) [54] resulted as the best compromise. A cyclic process of alternating 10% HF and water was also recommended, especially for the higher surface contaminant removal [60]. In Fig. 1 a XPS spectra comparison between an untreated Ge and a germanium treated with 5 cycles of 10% HF alternated with H_2O for 10 min clearly shows a net decrease in germanium oxide. The Ge–H termination is widely used, especially because of the high number of reactions that is possible to manage, but the stability of this termination is reported to be quite poor. As a matter of fact, S. Rivillon [61] and coauthors reported a 20% loss of –H after 1 min air exposure, caused by an initial exchange between hydrogen and hydrocarbon atoms. The initial loss of Ge–H termination leads to a CH_x contamination of the surface that is slowly replaced by a GeO_x growth. Fortunately, the Ge–H termination can be preserved in N_2 atmosphere, and it can be stable for more than 12h, even upon annealing to 100 °C.

Another germanium termination that can be easily reached is the sulfur passivation. The most used method is based on the use of $(NH_4)_2S$ aqueous solution after a HF pre-treatments [63,64]. Thanks to this process, a Ge–S termination is obtained from a freshly treated sample with a 5-min HF 2% treatment with a subsequent 30s long dip in a 20–25% $(NH_4)_2S$ solution. The reported stability of this passivation is higher than the Ge-H_x termination, starting from a 60% of surface coverage after the treatment, and reporting a slowly –S loss in the first 30 min and finally show a 2/3 –S loss after 120 min air exposure [64]. Other sulfur passivation techniques are reported in the literature, using H_2S chemisorption [65,66] and using $(NH_4)_2S$ but creating a GeS_x multilayer surface coating [67].

Germanium oxide removal can also be achieved by using a HCl acid treatment. The 10% HCl for 10 min treatment is used to reach a Ge-Cl_x termination with the removal of GeO_x by Sun and co-workers [68]. They reported a surface coverage of 0.8 ML, formed by 0.3 ML of mono-chloride and a 0.5 ML of di-chloride surface termination on Ge (100) surface, while Ge (111) forms only monochloride sites [69]. The residual surface coverage presents oxygen and carbon atoms, according
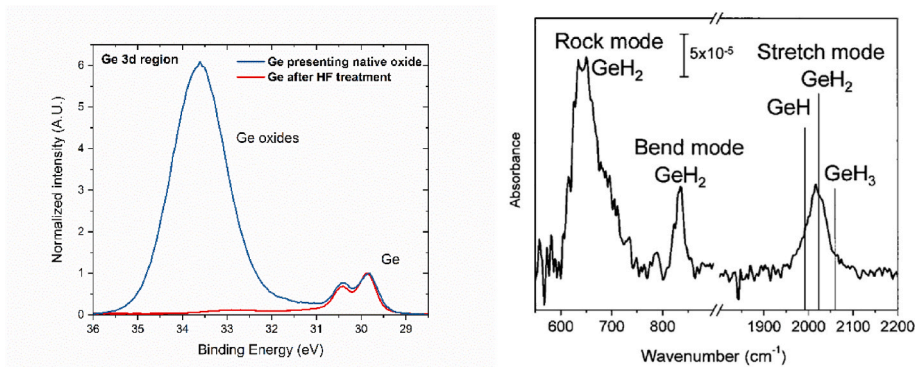

Fig. 1. On the left: XPS Ge (100) 3d region of an untreated Ge sample (blue spectrum) and a HF treated sample (red spectrum), by using 5 cycles of 10% HF and H_2O. The spectra are acquired with a photon energy equal to 350eV at Bach beamline, Elettra Synchrotron. On the right: transmission IRAS data of Ge (100) surface after 10 min 10% HF treatment. Mono- di- and tri-hydrate vibrational modes are indicated. Right image: Copyright 2005, AIP Publishing [54].

to photoelectron spectroscopy analysis. This procedure shows a similar behavior of HF removal procedure, since the 80% of surface metal contamination is reported to be cleaned by HCl dipping [70]. On the other hand, Park and co-workers [71] undertake another route for the creation of Ge–Cl termination, starting from a 10% HF surface treatment to obtain a Ge–H termination, and a subsequent 10% HCl treatment used to form Ge–Cl termination. Conversely to Ge–H case, the Ge–Cl termination cannot be easily revealed by infrared spectroscopy, since the Ge–Cl stretching signal is < 450 cm^{-1}, and only a lowering of Ge–H stretching signal can be revealed by FT-IR spectroscopy [71]. However, XPS measurements can directly reveal this termination and confirm the effectiveness of the treatment. In Fig. 2 a quantification of Ge–Cl termination is presented, revealing a clearly and quantifiable Rutherford backscattering Cl peak on a Ge sample obtained by following the Park et al. synthesis procedures. The revealed peak indicates a chlorine surface density (dose) equal to $4.5 \ 10^{14}$ cm^{-2}, that can be compared with a Ge (100) monolayer value, that is $6.25 \ 10^{14}$ cm^{-2}: considering a possible surface termination loss during the sample mounting (exposure in air for a few minutes), the effectiveness of the Ge–Cl generation is demonstrated, revealing that >0.7 ML is formed. The first application of Ge–Cl termination was demonstrated by Cullen et al. [72] by a reaction between ethyl Grignard reagent and the Ge–Cl termination, and others application will be further described in this paper.

In addition to these studied oxidant removal, there are a plethora of other studied that try different approaches [60]. As an example, a greener way to remove germanium oxide was discovered by Collins and coauthor [73] by using citric acid. This procedure was demonstrated to be effective by XPS analysis for the removal of germanium oxide, but comparing HCl and citric acid treatments, Heslop and coauthor [74] demonstrate a higher surface contamination coming from the citric treatment which could affect subsequent surface treatments. The reaction between citric acid and GeO$_x$ most likely generates a surface passivation formed by a mixture of species, composed by the product of citrate fragmentation [74,75]. This surface contamination can be diminished by reducing the concentration of citric acid below 1.2 M, but a lower oxide removal effectiveness is reported [74]. For this reason, this type of surface treatment is not recommended if a complete removal of Ge oxide and a good surface cleaning are needed.

3. Precursor adsorption and diffusion

Currently, numerous studies on monolayer doping of germanium have been published in the literature, exploring various approaches for self-limiting adsorption, dopant diffusion, and activation in Ge. The extensively researched monolayer doping MLD technique primarily focuses on n-type doping of germanium, benefiting from a wide range of molecular precursors available in the market, offering a broad choice of chemical functional groups. However, despite these efforts, n-type

doping of germanium is generally regarded as challenging, particularly when compared to conventional p-type doping. The main issues that commonly affect traditional germanium doping procedures are poor dopant activation, outgassing, and germanium desorption [76]. Moreover, the fast diffusivity of n-type species in germanium makes more difficult to create shallow junction on germanium, especially if a damage recovering post-annealing is needed after an ion-implantation process [77]. Indeed, the diffusion coefficient for n-type dopant $D_A(n)$ can be described by $D_A(n) = D_A(n_i) \ (n/n_i)$ [2] relation, where $D_A(n_i)$ is the intrinsic diffusivity and n_i the intrinsic carrier concentration at a given temperature. At high doping concentration $n > n_i$, the intrinsic diffusion coefficient $D_A(n_i)$ is amplified by the (n/n_i) [2] factor, significantly enhancing the diffusion of n-type species at relative high concentration, making more difficult to create an heavily doped shallow junctions.

The use of capping layer during the diffusion process is particularly interest for the maximization of the dopant level in the substrate. Several studies have been conducted on silicon substrates using SiO$_2$ oxide as a protecting layer, highlighting two main phenomena associated with the presence of a capping layer. The Si/Si oxide interface was found to be effective in trapping carbon contamination resulting from monolayer fragmentation, with retention of the native oxide layer being effective in trapping carbon contamination, a major concern in MLD techniques [78]. On the other hand, the use of a capping layer, aimed at improving doping efficiency, has been shown to be counterproductive: in certain cases, higher dopant yields may be achievable without applying such an oxide capping layer due to monolayer damage and trapping in the capping layer [79].

3.1. Phosphorus

The most extensively studied n-type doping approach for germanium is the use of phosphorus as a molecular precursor. Phosphorus is currently the standard n-type ion implantation dopant for Ge. However, it still faces certain challenges, such as achieving a low activation level after post-implantation annealing, typically below 50% of the total implanted dose [84].In the MLD case, the use of phosphorus-based molecules is facilitated by a large choice of molecular precursors in the market, which are normally non-toxic and low cost. Phosphorus can be found in a wide variety of molecules, starting from phosphorus oxides, phosphine oxide, phosphines, and each of them can presents different reactive functional groups. The most used functionalities are the reactive P–OH group and the P=O moiety that are the peculiar functional groups presented on phosphonic acids (both), phosphonates (P=O), phosphine oxides (P=O). As will be described in this paper, these moieties are reactive with germanium surfaces, and in particular with both Ge-OH and Ge–H surface terminations. As an alternative, the P–C–C≡C moiety can also be found on commercial precursors which could provide access to an hydrogermylation chemisorption [43] using
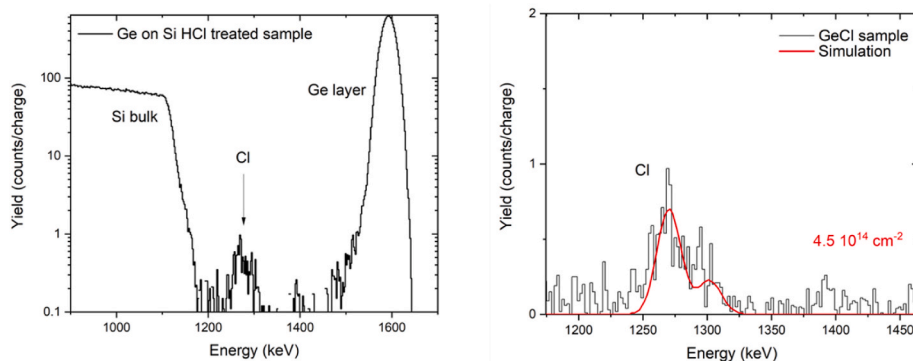

Fig. 2. On the left, Rutherford backscattering measurement of Ge thin film on Si after Ge–Cl synthesis (log y scale), as reported in the text. A Cl signal is clearly present and quantify by spectrum simulation (red curve superimposed to RBS spectrum on the right, linear y scale). The Cl surface density is estimated to be $4.5 \ 10^{14}$ atoms cm^{-2}.

the allyl functionality with Ge–H surface, but the presence of a reduced P in combination with the allyl group has not yet been previously tested.

The diethyl 1-propylphosphonate (DPP), the octadecylphosphonic acid (ODPA) and the allyldiphenyl phosphine (ADPP) are the molecular precursors used for n-type MLD in the literature [37,39,80]. These precursors are deposited on Ge by a wet monolayer doping by Sgarbossa et al. work [37], using a reflux system or a closed tube containing a mesitylene solution and the target material, and promoting the adsorption by heating the solution until the solution boiling temperature (Fig. 3). The Ge surface is pretreated with a HF 10% to remove the oxide and create a Ge–H surface termination as described in the previous section. Otherwise, Taheri and co-wokers [80] deposited the diethyl 1-propylphosphonate molecule by a gas phase deposition on a pre-treated Ge surface with only 0,5% HF solution for 5s, that allows to decrease the germanium oxide amount, but it does not ensure the formation of Ge–H superficial groups according to the literature [54,60, 61]. Therefore, the authors suggest a molecular chemisorption between DPP and Ge-OH functionalities, forming a P–O-Ge bridge starting from P=O and Ge-OH functional groups. According to the authors, the P=O moiety can act as a Lewis base, able to act as an electron donor for the –OH surface moiety, that act as a Lewis acid, accepting the electron.

Sgarbossa and co-authors also came to a similar conclusion [39]. However, their research emphasized a more intricate scenario regarding the adsorption process by comparing the behavior of DPP precursor with other different molecules presenting different functionalities, leading to a more comprehensive understanding of the adsorption mechanism [37]. As described in the previous section, the use of stronger HF treatment (10% HF cycled with water rising) enables the formation of Ge–H surface functionalities and minimizes the presence of surface oxide [54,60]. The subsequent deposition in mesitylene solution promotes a self-limited molecular adsorption with germanium, which involves the formation of both a chemisorbed and a physisorbed layers. This evidence emerges by an accurate ion beam analysis that allows to quantify the phosphorus atomic dose. In agreement with Taheri work, DPP seems to form a P–O-Ge bond to the surface [39], but the global dose of P detected on the surface of the sample suggest that the surface

density of molecule can vary depending on the deposition ambient [37]. As a matter of fact, the same adsorption procedure carried out inside a dry-box instead of using a standard ambient reduced the adsorbed surface density from about 4 ML to 1 ML, thus suggesting that the physisorption is enhanced (or caused) by the presence of trace of humidity. Interestingly, both treatments show a self-limiting and a reproducible behaviour, as demonstrated by several samples analyzed [37].

An interesting observation is the correlation between a slight increase in germanium oxide and the strongly physisorbed fraction, particularly in samples without dry conditions. This phenomenon is observed for both phosphonate (DPP) and phosphonic acid (ODPA) molecules. This behavior aligns with the interpretation of the interaction between these molecules and the surface: the physisorbed fraction arises from the short-range interaction between germanium oxide and the molecule P=O moieties. Furthermore, non-dry adsorption not only leads to an increase in the surface density of phosphorus and germanium oxide but also introduces physisorption inhomogeneity. This inhomogeneity becomes apparent through SIMS analysis performed on different positions of the sample after the in-diffusion process. The authors propose that the growing amount of inhomogeneous physisorbed phosphorus fraction is likely attributed to the presence of localized spots of germanium oxide formed on the sample surface. These spots induce a local increase of physisorption of the molecular precursor on top of them due to the favorable interaction between them.

A third phosphorus-based precursor is analyzed, the allyl-diphenyl phosphine (ADPP) [37], presenting a complete different reactive site: the allyl group. The chemisorption of this molecule on Ge–H surface is expected to follow a different reaction pathway compared with the previous scenarios, thus forming a Ge–CH$_2$–CH$_2$-CH$_2$-P bridge through an hydrogermylation reaction mechanism [43]. As shown by Sgarbossa and co-authors [37], the molecular chemisorption occurs under both in dry and ambient conditions, albeit through different reaction paths. Oxidation of the phosphorus-based molecule occurs, resulting in the formation of two new phosphorus-oxygen bonds with the surface. The authors suggest that the hydrogermylation reaction is less favored in these conditions, while phosphorus oxidation becomes more favored, primarily due to the presence of the germanium surface. This unexpected behaviour is supported by several experimental investigation, such as infrared spectroscopy, XPS and EXAFS analysis, suggesting a facile phosphorus oxidation on germanium surface. This ultimately results in the formation of a self-limited monolayer, exhibiting this behaviour both on dry and ambient conditions.

These molecules are finally tested as dopant sources, revealing different diffusion attitudes based on their adsorption process. Sgarbossa and co-workers [39] were unsuccessful in the attempt to reveal a phosphorus in-diffusion on germanium by using standard and rapid thermal annealing, demonstrating that the entire phosphorus remains at the interface in between Ge and capping. This lack of diffusion suggests that the used annealing was insufficient to provide a thermal budget able to properly fragment the molecular precursors. This happens in spite the explored thermal budget was particularly wide, ranging from 650 °C for 60s up to 825 °C for 5min for DPP and ODPA molecules.

On the other hand, by using an out of equilibrium process, these surface dopant sources are revealed to be effective. Pulsed Laser Melting (PLM, previously also called Laser Thermal Annealing) [85] can be successfully used on DPP, ODPA and ADPP molecular sources, promoting the fragmentation and the in diffusion of atomic species [37,39]. The sample irradiation using an UV nanosecond laser pulse induce a controlled surface heating that induce a superficial Ge melting and promote a molecular fragmentation. Sgarbossa and co-authors have deduced from thermal budget calculations that a direct contribution of UV photon absorption on the adsorbed molecules must come into play in order to promote molecular fragmentation. Indeed, the molecule's heating alone following the melting of germanium for such a short period should not be sufficient to provide the energy required for complete molecular fragmentation.
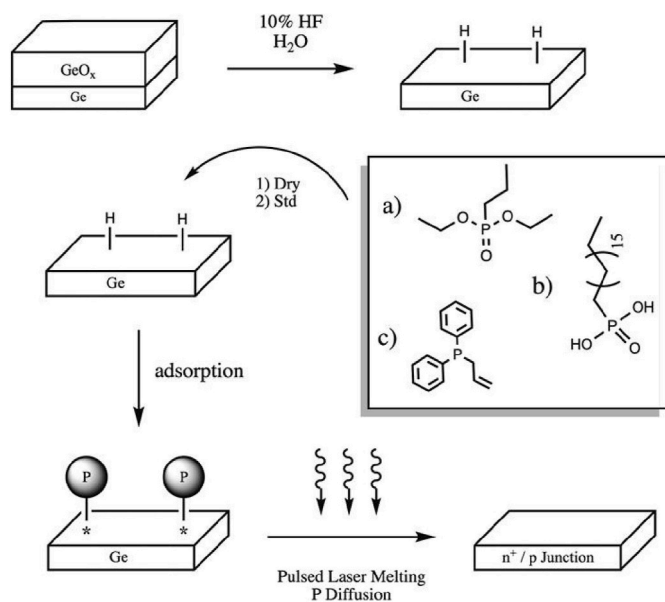

Fig. 3. Schematic representation of ML deposition process used by Sgarbossa and co-workers for the phosphorus MLs deposition on Ge. After the surface preparation with a HF treatment (on top), three different molecular precursors are tested as phosphorus sources, using two different deposition procedures, called standard (std) and dry processes. The diffusion of dopant is obtained by using pulsed laser melting technique as described in the text. Copyright 2020, Elsevier Ltd [37].

It is important to emphasize that the n-type precursors used, such as DPP and ODPA, possess stable P–O- and P=O bonds, typically presenting a dissociation energy of 340 and 540 Kj/mol [86,87] (3.6 eV, 5.6 eV) respectively. The energy required for monolayer dissociation can be estimated to fall in between these values [37], depending on the type of the adsorption that takes place. This suggests that a significant amount of energy is needed for the molecular bond dissociation, which is a crucial step in releasing atomic P species, as discussed in Ref. [39]. DPP and ODPA molecules have proven to be effective for MLD on silicon, as demonstrated in the literature [88], exhibiting similar surface adsorption characteristics on Si substrate. However, the lower diffusion temperature required for germanium substrate imposes limitations on the thermal budget available for molecular fragmentation. Typically, a thermal window of 900–1100 °C can be utilized for Si substrates, whereas for Ge it is reduced and lowered to 600–800 °C. This significant difference could be one of the reasons why achieving effective phosphorus diffusion and activation on Ge is more challenging, assuming the same treatments timescale. By employing pulsed laser melting techniques, the temperature of Ge can be raised to at least Ge melting point (937 °C) but the thermal budget is now limited by the short duration of the process (hundred(s) of ns) compared to rapid thermal annealing.

Finally, once the phosphorus atoms have been released, they are free to diffuse into the Ge liquid phase. Due to the high diffusion coefficient in the liquid phase, these atoms can readily move and spread throughout the material, leading to the formation of a highly doped thin region. The crystallinity of the melted layer is fully restored by epitaxial regrow, which occurs after a certain delay required for the heat dissipation process.

In Fig. 4 SIMS profiles of phosphorus doped germanium after PLM (KrF excimer laser using an energy density of 500 mJ cm^{-2} with a pulse duration of 22 ns) using ADPP molecular surface is shown, exploiting the role of the number of laser pulses to diffuse phosphorus from a surface molecular source. Four-point electrical measurements were performed on ADPP functionalized Ge surface after 12 pulses (green line), revealing
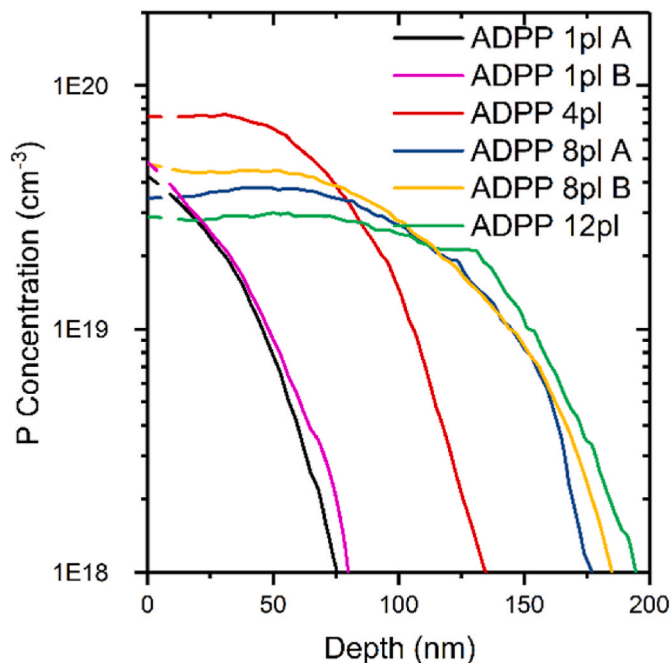
a sheet resistance of 52 Ω/□, compared to >700 Ω/□ of the bulk undoped sample, reveals a high electrical activation of the diffused dopant, reported to be compatible with a fully electrical activation.

Taheri and co-workers present a different perspective [80], showing an effective thermal in diffusion for DPP precursor by investigating the sheet resistance of Ge processed sample with rapid thermal annealing at 600, 650 and 700 °C for less than 3 min. The results shown in Fig. 5 reveal a drop-in sheet resistance from 1000–1200 Ω/□ to 200–600 Ω/□, depending on the treatment temperature. Unfortunately, there is no SIMS data for Ge doping case, which makes difficult to evaluate the effectiveness of the process and the activation level of the dopant. The two different results obtained for the same molecule DPP, suggest that the different deposition procedure plays a role.

Taheri et al. suggest that DPP chemisorbs onto the surface via P–O-Ge moiety following a gas-phase deposition. This is achieved by exposing the Ge-OH termination to DPP precursor and a mild heating, indicating the greatest surface density of P obtained at 95 °C. Similarly, Sgarbossa et al. achieved the P–O-Ge molecular bond grafting using a wet chemical deposition at 164 °C on Ge–H surface termination but highlighting the role of the water on increasing the adsorbed P surface density. In both studies, the sample were capped with a SiO$_2$ layer to act as an out-diffusion barrier during rapid thermal processing.

It is important to note that Sgarbossa et al. exclusively tested thermal diffusion using the wet deposition approach, while Taheri et al. utilized only dry gas-phase deposition process. The discrepancy in the results could potentially be attributed to the different deposition methods employed, even if it is unusual for the same molecule, bound to the surface via the same bond, to exhibit such divergent diffusive behaviors. It is plausible to considered that an RTA process on Sgarbossa et al. samples could be effective to form a shallow junction for the dry synthesis process.

A possible alternative scenario could be related with the electrical measurement of Taheri and co-workers: the reduction in sheet resistance observed on the Ge sample could be due to the diffusion of contaminant atoms diffused from the surface into the bulk [89], thus lowering the surface electrical resistance but not indicating a phosphorus activation. Further test and analyses should be carried on clarifying the effectiveness of rapid thermal annealing to cleave the stable Ge-O-P bond and release P for the in-diffusion, considering the role of water traces in these

Fig. 4. SIMS of phosphorus in germanium after pulsed laser melting diffusion process on ADPP precursor at 500 mJ cm^{-2}. Different number of laser pulses are analyzed, exploiting the surface release and diffusion of P, and different profile on different place on the same sample (ADPP 1 pl A, B and 8 pl A, B) demonstrate the lateral uniformity of the doping process. Copyright 2020, Elsevier Ltd [37].
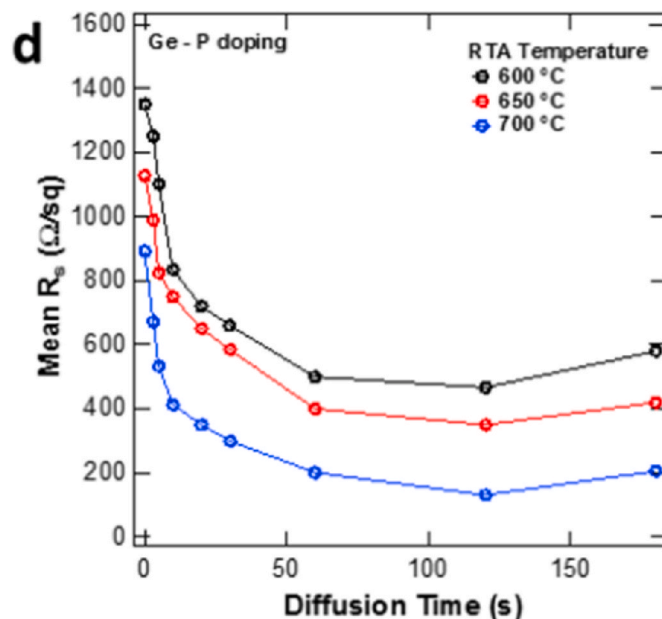
Fig. 5. Vales of sheet resistance as a function of the duration of rapid thermal annealing process on DPP functionalized samples. Copyright 2017, American Chemical Society [80].
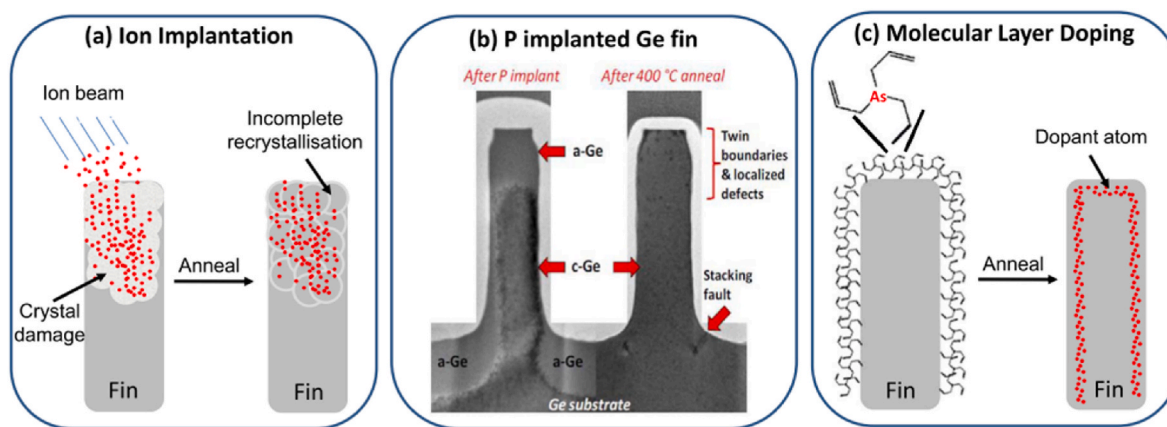
Fig. 6. Schematic representation of Long and co-workers' process for the Fin doping using arsenic MLD sources. In the a) panel, the associated problems regarding the ion implantation on Fin nano-structures; b) a cross section TEM performed on Ge Fin after the ion implantation process, highlighting the residual ion implanted defects; c) a schematic representation of As MLD on Ge Fin. Copyright 2017, Elsevier Ltd [40].

surface processes.

3.2. Arsenic

The second n-type dopant that has been investigated for MLD on Ge is arsenic. As is commonly used as dopant for Ge using the ion implantation technique [90,91], but it exhibits incomplete damage recovering after the post annealing. This results in a residual concentration of defects that acts as acceptors, thereby compensating for the electrical activity of implanted As. To overcome this limitation, alternative approaches have been explored in the literature, such as a Gas phase doping of Ge using As [92]: it offers a lower defects concentration and a higher dopant activation compared to ion implantation, but it forms a junction with a micron-scale depth. Another promising strategy is the use of ion implantation in combination with pulsed laser melting as a damage recovering technique which increasees the activation of ion implanted As up to $1 \; 10^{20} \; cm^{-3}$ thanks to the melting and recrystallization of the doped layer [93].

A major challenge associated with the use of As is it toxicity, which has led to a rare utilization in various MLD studies [82]. In addition, the limited availability of suitable As precursors in the market has necessitated the synthesis of precursors specifically for MLD applications. Despite these complications, As has been successfully employed for MLD technique, using the triallyl arsine synthetized starting from the commercially available arsanilic acid. It is worth noting that arsenic exhibits relatively high equilibrium solubility compared to other n-type dopants, making it a favorable choice in certain cases.

Long et al. have published two studies regarding on arsenic monolayer doping of germanium [40,81] using the triallyl arsine (TAA) as the precursor. In their approach, the TAA is chemisorbed onto germanium after a 10-min treatment with a 10% HF solution. To avoid molecular thermal degradation at high temperatures, an UV-irradiated hydrogermylation reaction was employed instead of standard thermal adsorption process, as previously tested on Si [94]. Both chemisorption and physisorption occur during the treatment, and a rinsed procedure is found effective for the physisorbed fraction removal. Following the deposition of a SiO2 capping layer to prevent arsenic out-diffusion, rapid thermal annealing at 650 °C for various durations (1, 10, 100 s) was used for molecular thermal decomposition and diffusion in germanium. The highest active carrier concentration was reported to be $6.0 \; 10^{18} \; cm^{-3}$, as extracted by ECV measurements. Long and co-worker's noted that varying the thermal budget did not result in a significant variation of the peak concentration, suggesting that the process had already reached the solubility limit of As in Ge at 650 °C.

In a subsequent study by the same group [40], a wider thermal range

was explored using rapid thermal annealing. However, no active carrier concentration higher than $6.0 \; 10^{18} \; cm^{-3}$ was achieved, confirming the previous solubility limit. This work also demonstrated for the first time the efficacy of arsenic MLD on germanium nanowires (Fig. 6), showing successful nanostructure doping. Electrical measurements on the nanowires exhibited variations in conductivity, further confirming the efficacy of the MLD technique on germanium nanostructures. In addition, the study investigated the use of capping layers and found that the deposition of a SiO2 layer could be avoided, as similar results were obtained with sputtered, CVD, evaporated, and no SiO2 capping layers.

In a recent study by Kennedy et al. [82], a new method for As MLD on Ge surfaces was explored using an arsanilic acid as the As molecular precursor. The Ge surface were pre-treated with a solution of HCl 10% for 10 min, leading to the formation of a hydrophilic Ge–Cl surface termination. The arsanilic acid was then chemisorbed on to the surface by using a tethering by aggregation (T-BAG) deposition method, involving an annealing at 140 °C for 10h in a vacuum oven. The molecular precursor reacts with the surface Ge–Cl termination and most likely forms As–O-Ge bond. The authors also suggest the possibility of Ge–(NH)–R chemisorption based on a computed negative adsorption energy of −3,66 eV, which can be compared to −4,97 eV and −5,70 eV for bi- and mono-chemisorption via As–O-Ge bonds. Rapid thermal annealing in between 400 and 700 °C and 1–100s were performed after a SiO2 capping deposition, revealing the possibility to dope germanium with an As active concentration of approximately $10^{19} \; cm^{-3}$ (Fig. 7), achieving higher value than previous works. This level of active concentration makes As MLD a potential technique for FET channels materials. Furthermore, the use of arsanilic acid simplify the realization of arsenic MLD as the precursor is commercially available and is more stable with respect triallyl arsine precursor.

3.3. Antimony

The monolayer doping technique has recently been extended to antimony, increasing the possibility to obtain the n-type doping also with this bulky dopant atom. It is widely known in the literature that ion implantation is more damaging for larger dopants such as Sb, which poses challenges for achieving shallow junctions [95]. For this reason, the semiconductor industries requiring new doping technique for the use of Sb as Ge dopant. Furthermore, the use of Sb as Ge dopant is gaining traction due to its ability to induce a high level of strain within Ge material. This feature makes the study of antimony incorporation particularly interesting for germanium bandgap engineering, adding to the appeal of utilizing antimony as a germanium dopant [96].

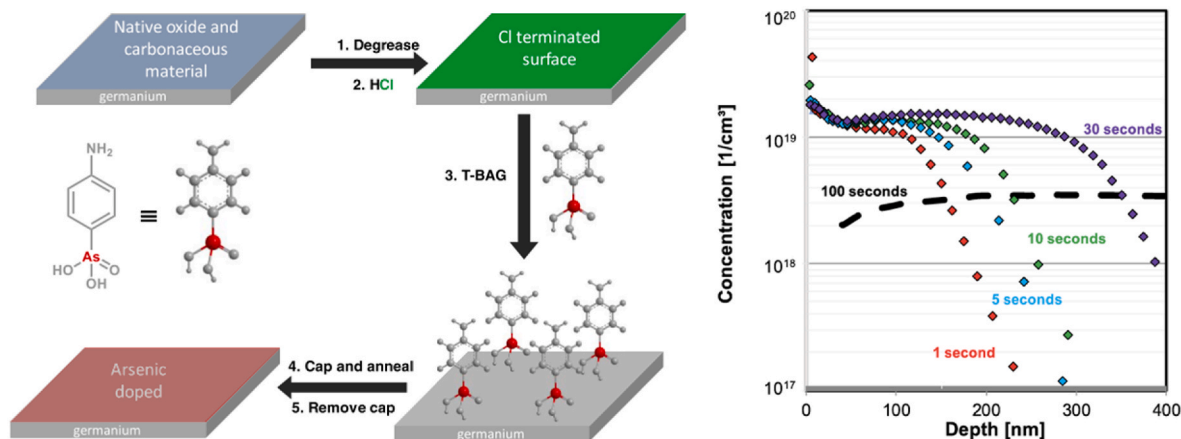Alphazan and co-authors addressed the challenge of Sb monolayer

Fig. 7. On the left, a schematic representation of Kennedy and co-workers' process for the formation of arsanilic acid monolayer on germanium surface. On the right, ECV activation measurements of As in Ge after RTA process at 650°C using a SiO$_2$ capping. Both image Copyright 2020, American Chemical Society [82].

doping by utilizing an oligomeric molecule containing Sb, the hepta-isobutyl polyhedral oligomeric solsesquioxane antimony trimester (POSS–Sb), as a diffusion source of Sb. The germanium surface underwent a pretreatment with citric acid, as discussed in the previous section, resulting in the formation of various species that passivated the germanium surface and created different surface terminations. The authors suggested that chemisorption likely occurred due to the reactivity of the –OH surface group formed by the adsorbed citric acid and the POSS-Sb molecule. Surface characterization revealed that the adsorbed layer exhibited a Sb/Si ratio approximately seven times lower than the expected stoichiometric ratio of the unreacted precursor: this discrepancy highlighted significant molecular reassembly during the adsorption process, which the authors attribute to the occurred surface chemisorption.

To prevent the sublimation of Sb during the subsequent annealing process, the adsorbed POSS-Sb was capped by a SiO$_2$ protective layer. The annealing process was performed using a rapid thermal annealing process with an initial step at 550 °C for 10 min, followed by a temperature increase to 600 °C for 10s. The electrical activation of the dopant was evaluated by a four-point probe test, which revealed an active concentration in the range 10^{20}–10^{21} cm^{-3}. However, the measurement was obtained with a tip spacing smaller than 20 μm, raising concerns about the lateral homogeneity of the electrical activation/diffusion processes. SIMS measurements posed challenges due to the expected junction depth of 10–20 nm, which falls within the SIMS artifact region caused by the non-steady state sputtering process. This results in a slow trailing slope due to significant mass transport of high mass elements such as Sb. Despite the difficulties in quantification, a comparison between non-treated and annealed samples showed an increase in Sb signal, suggesting diffusion of Sb within the material.

An alternative method for antimony-based germanium doping has been proposed by Sgarbossa and co-authors [37]. Instead of depositing the molecular precursor directly on Ge surface by wet chemistry, Sb is deposited through gas phase deposition [97]. In a fluxed N$_2$ atmosphere, an antimony source sample and an untreated Ge target material are heated in between 600 and 780 °C. In this temperature range, metallic Sb sublimes from the source material (a sputtered thin film deposited on silicon) and is deposited on Ge surface, as illustrated in Fig. 8. In this temperature range, the deposition on the Ge (100) surface exhibits a self-limiting behavior, resulting in the formation of 1 ML of antimony. Furthermore, the Sb deposition on Ge occurs with minimal germanium oxide formation, as GeO$_x$ sublimes from the surface in this temperature range. On the contrary, at lower temperatures Sb can still be deposited on germanium, but the self-limiting behavior is absent, underlining the importance of the germanium oxide sublimation process for Sb monolayer formation. Based on these observations, the authors propose a chemisorption mechanism involving the oxidation of Sb$_4$ gas to form an Sb oxide monolayer and the reduction of GeO to Ge.

After the surface studies, the Sb monolayer is tested as a dopant source. Standard and rapid thermal annealing are performed, showing that only the 4% of the total Sb dose revealed by RBS measurements is available for in-diffusion in Ge matrix. This small percentage is compatible with synchrotron XPS result, that revealed a small Sb metallic fraction below the Sb oxidized surface monolayer. Apparently only this fraction can diffuse inside Ge, forming a fully active junction with a concentration in the rage of 4–5 10^{18} cm^{-3} at 615 °C for 20s. In contrast, all the oxidized antimony is not available for in-diffusion in Ge. However, by employing pulsed laser melting technique, all the Sb monolayers can be made available for germanium in diffusion, resulting in a fully electrical active junction (Fig. 8, right side) with a
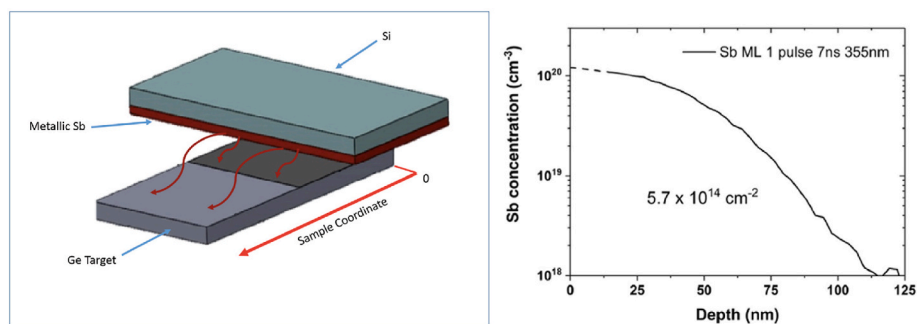

Fig. 8. On the left, schematic representation of gas phase deposition of Sb monolayer from a sputtered Sb layer on Si source. On the right, SIMS profile of Sb in Ge diffused with pulsed laser melting technique. Both image Copyright 2019, Elsevier Ltd [53].

concentration exceeding 10^{20} cm^{-3}, as verified by four probe electrical measurements on a macroscopical area $0,5 \times 0,5$ cm [2]. Building upon these findings, Carraro and co-workers [96] further explore Sb doping in germanium using a sputtering Sb deposition in combination with PLM, demonstrating the possibility of incorporating more than 10^{22} cm^{-3} of Sb in Ge and reaching a maximum active concentration of 3 10^{20} cm^{-3}. Although this methodology is not self-limiting, it reveals that Sb GP MLD already reached a value very close to the maximum achievable active concentration using PLM, i.e. an active concentration of 10^{20} cm^{-3}.

3.4. Boron

The only study addressing p-type doping of germanium using the MLD technique is conducted by Taheri and co-workers [80], employing the Allylboronic acid pinacol ester (ABAPE) as precursor. Similar to the n-type gas phase deposition method mentioned earlier, the ABAPE precursor is introduced into a reactor under a flux of gas, with the reactor heated between 70 and 120 °C and a Ge target pretreated with 0.5% HF water solution for 5s is used. The authors observe the formation of R-C-C-Ge grafting as a consequence of the reaction between ABAPE and Ge-OH surface groups. The authors observe the formation of a R-C-C-Ge grafting, indicating the reaction between ABAPE and Ge-OH surface groups. This reaction between the –OH group and the carbon double bond is inferred from the absence of C=C stretching vibration post-deposition, together with the appearance of a broad C–O vibrational mode present in the ABAPE molecular structure. XPS analysis reveals a decrease in the O1s signal attributed to –OH moiety, while the O1s attributed to the B–O is increasing. This experimental evidence supports the chemisorption of the precursor and suggest a Ge-OH + C=C–R → Ge-C-C-R as the most likely reaction mechanism. The maximum deposited density of precursor is observed at 95 °C, while the amount of precursor decreases at higher and lower temperatures. This behavior suggests a thermally activated process and the increase in deposition rate correlates with a higher thermal molecular energy.

Thermal diffusion tests conducted in the temperature range of 600–700 °C demonstrate a decrease in sheet resistance on Ge sample, as shown in Fig. 9 (right side). However, the paper does not provide direct evidence of boron chemical profile within germanium or information regarding the doping type (p or n type) coming from electrical activation measurements.

These results leave many doubts on the effective diffusion and electrical activation of B: it is well established that B is one of the doping species with lower diffusivity in germanium [98] presenting an activation energy as high as 4.6 eV. As a matter of fact, the diffusion length expected under the reported experimental condition is easily

computable, resulting in a length less than a fraction of nm. In particular, for the lower reported sheet resistance obtained with 700 °C for 120s thermal treatment, the estimated diffusion length for boron in germanium is 0.1 nm. The above consideration allows to dubitate that the decrease on sheet resistance can be attributed to a B activation rather than a contaminant atom; this suggest that further investigation is required to determine the real reason for the reduction in sheet resistance.

4. Conclusions

This paper reviews the progress of the monolayer doping technique in germanium and show that significant improvements have been made in recent years, making this new doping technique effective for germanium as well as silicon. Compared to Si, germanium has a more complex surface dynamics and a poor surface chemical passivation stability. The commonly used surface terminations exhibit low air stability, and when combined with the easily air germanium surface oxidation, achieving proper germanium surface termination becomes challenging. Consequently, the adsorption of molecular precursors onto germanium surfaces is complicated and requires appropriate surface preparation.

N-type doping of germanium using monolayer doping has been explored extensively, utilizing precursors with suitable functional groups for P, As, and Sb doping. However, literature reports only one work on p-type doping, which employs a boron precursor. We express doubts regarding the efficiency of this method due to a lack of data and an incongruence of boron diffusion in germanium with the well-known literature diffusivity. Further investigations should be conducted on p-type doping, potentially considering other dopants such as gallium.

Different MLD approaches have been successfully tested, including classical monolayer doping and gas phase monolayer doping. In most cases, Ge-O-Dopant bond is formed after the adsorption process, while using proper precursors, such as TAA or ABAPE, a Ge-C-C-Dopant chemisorption is reported to be formed. Most of the studies require a dry deposition, using a vacuum or inert gas phase deposition in a dry box ambient to preserve the surface germanium functionalization and avoiding a re-oxidation of the germanium surface. The molecular fragmentation and the subsequent dopant diffusion in Ge were obtained exploiting rapid thermal annealing or using pulsed laser melting technique. The higher dopant concentrations are obtained by using the pulsed laser melting technique, revealing its ability to promote a complete in-diffusion of dopant, and having as an added benefit the non-use of a capping layer. In some cases, the Ge-O-Dopant bond is not decomposed by means of conventional or rapid thermal annealing, instead laser processing successfully provides reduced dopant atoms for doping.
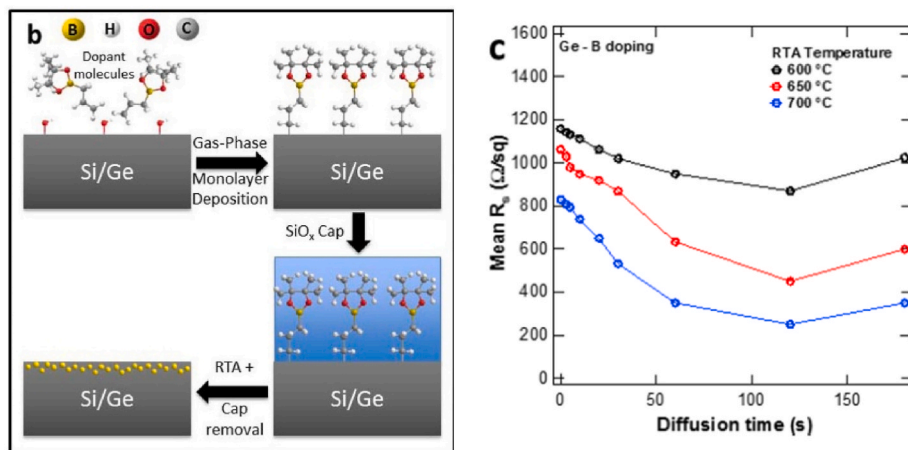

Fig. 9. On the left, a schematic representation of ABAPE monolayer deposition process in Taheri work. On the right, sheet resistance measurements obtained after ABAPE diffusion treatment in Ge. Both image Copyright 2017, American Chemical Society [80].

This may be attributed to the higher temperature reached during the process (close to the substrate melting temperature), and/or the ability of UV light to produce molecular fragmentation as a consequence of a direct interaction between photons and the adsorbed monolayer [39]. Further investigation is required to clarify and investigate this intriguing point. The role of capping layers is another important key aspect that deserves to be investigated in depth: it is unclear if the SiO_2/Ge interface can efficiently trap carbon atoms during the fragmentation process as in Si case, especially if we considered the different formation tendency of Si–C and Ge–C bonds [62].

Unfortunately, pulsed laser melting poses challenges when applied to nanostructured materials due to material melting caused by the laser pulse. Consequently, this technique cannot be applied to 3D nano-structures until effective solutions are developed. Currently, there is ongoing research on the integration of laser annealing and pulsed laser melting into complementary metal-oxide-semiconductor (CMOS) and 3D devices, with recent literature indicating a strong industry effort toward their actual implementation in device manufacturing [99].

Several improvements to Ge MLD are still possible, starting with the use of different diffusion processes, such as flash lamp annealing, that might improve the dopant release, confining the dopant species in the first nanometers of germaniums. Although several scientific works have been published on monolayer doping in germanium, many issues are still to be clarified and many approaches and techniques have yet to be tested in germanium, such as monolayer contact doping.

Copyrights agreements

Fig. 1b: reprinted from "Rivillon, S., Chabal, Y. J., Amy, F., & Kahn, A. (2005). Hydrogen passivation of germanium (100) surface using wet chemical preparation. *Applied Physics Letters*, *87*(25), 1–3", with the permission of AIP Publishing.

Figs. 3 and 4: reprinted from publication: Sgarbossa, F., Levarato, A., Carturan, S. M., Rizzi, G. A., Tubaro, C., Ciatto, G., … De Salvador, D. (2020). Phosphorus precursors reactivity versus hydrogenated Ge surface: towards a reliable self-limited monolayer doping. *Applied Surface Science*, *541*(148532). Copyright (2020) with permission from Elsevier.

Figs. 5 and 9: reprinted with permission from: Taheri, P., Fahad, H. M., Tosun, M., Hettick, M., Kiriya, D., Chen, K., & Javey, A. (2017). Nanoscale Junction Formation by Gas-Phase Monolayer Doping. *ACS Applied Materials and Interfaces*, *9*, 20648–20655. Copyright (2017) American Chemical Society.

Fig. 6: reprinted from publication: Long, B., Alessio Verni, G., O'Connell, J., Shayesteh, M., Gangnaik, A., Georgiev, Y. M., … Holmes, J. D. (2017). Doping top-down e-beam fabricated germanium nanowires using molecular monolayers. *Materials Science in Semiconductor Processing*, *62*, 196–200. Copyright (2017) with permission from Elsevier.

Fig. 7: reprinted with permission from: Kennedy, N., Garvey, S., MacCioni, B., Eaton, L., Nolan, M., Duffy, R., … Long, B. (2020). Monolayer Doping of Germanium with Arsenic: A New Chemical Route to Achieve Optimal Dopant Activation. *Langmuir*, *36*(34), 9993–10002. Copyright (2020) American Chemical Society.

Fig. 8: reprinted from publication: Sgarbossa, F., Maggioni, G., Rizzi, G. A., Carturan, S. M., Napolitani, E., Raniero, W., … De Salvador, D. (2019). Self-limiting Sb monolayer as a diffusion source for Ge doping. *Applied Surface Science*, *496*, 143713. Copyright (2019) with permission from Elsevier.

CRediT authorship contribution statement

Francesco Sgarbossa: Writing – original draft, Formal analysis, Data curation, Conceptualization.

Declaration of competing interest

The authors declare that they have no known competing financial interests or personal relationships that could have appeared to influence the work reported in this paper.

Data availability

Data will be made available on request.

Abbreviations

MLD	monolayer doping
TAA	triallyl arsine,
DPP	diethyl 1-propylphosphonate
ODPA	octadecylphosphonic acid
ADPP	allyldiphenyl phosphine,
ABAPE	Allylboronic acid pinacol ester
POSS-Sb	hepta-isobutyl polyhedral oligomeric solsesquioxane antimony trimester
MLCD	monolayer contact doping
rMLD	remote monolayer doping
GP-MLD	gas phase monolayer doping

References

[1] M. Leong, B. Doris, J. Kedzierski, K. Rim, M. Yang, Silicon device scaling to the sub-10nm regime, Science 306 (2004) 2057–2060 (80*)*.

[2] M. Waldrop, More then Moore, Nature 530 (2016) 145.

[3] E. Simoen, et al., Ion-implantation issues in the formation of shallow junctions in germanium, Mater. Sci. Semicond. Process. 9 (2006) 634–639.

[4] R. Pillarisetty, Academic and industry research progress in germanium nanodevices, Nature 479 (2011) 324–328.

[5] K.P. Homewood, M.A. Lourenço, The rise of the GeSn laser, Nat. Photonics 9 (2015) 78–79.

[6] Z. Zhou, B. Yin, J. Michel, On-chip light sources for silicon photonics, Light Sci. Appl. 4 (2015) 1–13.

[7] P. Chaisakul, et al., Integrated germanium optical interconnects on silicon substrates, Nat. Photonics 8 (2014) 482–488.

[8] J. Van Der Heide, N.E. Posthuma, G. Flamand, J. Poortmans, Development of low-cost thermophotovoltaic cells using germanium substrates, AIP Conf. Proc. 890 (2007) 129–138.

[9] S. Bertoldo, et al., New method for the production of thin and stable , segmented n + contacts in HPGe detectors, Eur. Phys. J. A 57 (2021) 1–10.

[10] G. Maggioni, et al., Pulsed laser di ff usion of thin hole-barrier contacts in high purity germanium for gamma radiation detectors, Eur. Phys. J. A 54 (2018).

[11] A.I. Yakimov, et al., Photovoltaic Ge/SiGe quantum dot mid-infrared photodetector enhanced by surface plasmons, Opt Express 25 (2017), 25602.

[12] J. Oh, et al., Interdigitated Ge p-i-n photodetectors fabricated on a Si substrate using graded SiGe buffer layers, IEEE J. Quant. Electron. 38 (2002) 1238–1241.

[13] K. Washio, et al., A 0.2-μm 180-GHz-f max 6.7-ps-ECL SOI/HRS self-aligned SEG SiGe HBT/CMOS technology for microwave and high-speed digital applications, IEEE Trans. Electron. Dev. 49 (2002) 271–278.

[14] K. Oda, E. Ohue, M. Tanabe, H. Shimamoto, K. Washio, Si1-xGex selective epitaxial growth for ultra-high-speed self-aligned HBTs, Thin Solid Films 369 (2000) 358–361.

[15] J. Frigerio, et al., Tunability of the dielectric function of heavily doped germanium thin films for mid-infrared plasmonics, Phys. Rev. B Condens. Matter 94 (2016) 1–18.

[16] M.J. Süess, et al., Analysis of enhanced light emission from highly strained germanium microbridges, Nat. Photonics 7 (2013) 466–472.

[17] J.R. Sánchez-Pérez, et al., Direct-bandgap light-emitting germanium in tensilely strained nanomembranes, Proc. Natl. Acad. Sci. U.S.A. 108 (2011) 18893–18898.

[18] N.W. Hendrickx, D.P. Franke, A. Sammak, G. Scappucci, M. Veldhorst, Fast Two-Qubit Logic with Holes in Germanium, 2019, https://doi.org/10.1038/s41586-019-1919-3.

[19] N.W. Hendrickx, et al., A four-qubit germanium quantum processor, Nature 591 (2021).

[20] IEEE. IRDS More Moore. (2020) 1–30.
[21] J.C. Ho, et al., Controlled nanoscale doping of semiconductors via molecular monolayers, Nat. Mater. 7 (2008) 62–67.
[22] S. Yitzchaik, R. Gutierrez, G. Cuniberti, R. Yerushalmi, Diversification of device platforms by molecular layers: hybrid sensing platforms, monolayer doping, and modeling, Langmuir 34 (2018) 14103–14123.
[23] O. Hazut, et al., Contact doping of silicon wafers and nanostructures with phosphine oxide monolayers, ACS Nano 6 (2012) 10311–10318.
[24] O. Hazut, R. Yerushalmi, Direct dopant patterning by a remote monolayer doping enabled by a monolayer fragmentation study, Langmuir 33 (2017) 5371–5377.
[25] L. Ye, et al., Controlling the dopant dose in silicon by mixed-monolayer doping, ACS Appl. Mater. Interfaces 7 (2015) 3231–3236.
[26] J. O'Connell, et al., Organo-arsenic molecular layers on silicon for high-density doping, ACS Appl. Mater. Interfaces 7 (2015) 15514–15521.
[27] J.O. Connell, S. Biswas, R. Duffy, Chemical approaches for doping nanodevice architectures, Nanotechnology 27 (2016).
[28] J.C. Ho, et al., Wafer-scale, sub-5 nm junction formation by monolayer doping and conventional spike annealing, Nano Lett. 9 (2009) 5–10.
[29] J. Veerbeek, et al., Highly doped silicon nanowires by monolayer doping, Nanoscale 9 (2017) 2836–2844.
[30] J. Veerbeek, J. Huskens, Applications of monolayer-functionalized H-terminated silicon surfaces: a review, Small Methods 1 (2017), 1700072.
[31] T. Alphazan, et al., Monolayer doping of silicon through grafting a tailored molecular phosphorus precursor onto oxide-passivated silicon surfaces, Chem. Mater. 28 (2016) 3634–3640.
[32] S.S. Chuang, et al., Ultra-shallow junction formation by monolayer doping process in single crystalline Si and Ge for future CMOS devices, ECS J. Solid State Sci. Technol. 6 (2017) P350–P355.
[33] K.W. Ang, et al., 300mm FinFET results utilizing conformal, damage free, ultra shallow junctions (X j~5nm) formed with molecular monolayer doping technique, Tech. Dig. - Int. Electron Devices Meet. IEDM (2011) 837–840, https://doi.org/10.1109/IEDM.2011.6131679.
[34] R. Yerushalmi, J.C. Ho, Z. Fan, A. Javey, Phosphine oxide monolayers on SiO 2 surfaces, Angew. Chem. 120 (2008) 4512–4514.
[35] E. Arduca, et al., Synthesis and characterization of P δ -layer in SiO 2 by monolayer doping, Nanotechnology 27 (2016), 75606.
[36] N. Kennedy, et al., Phosphorus monolayer doping (MLD) of silicon on insulator (SOI) substrates, Beilstein J. Nanotechnol. 9 (2018) 2106–2113.
[37] F. Sgarbossa, et al., Phosphorus precursors reactivity versus hydrogenated Ge surface: towards a reliable self-limited monolayer doping, Appl. Surf. Sci. 541 (2021).
[38] F. Sgarbossa, et al., Self-limiting Sb monolayer as a diffusion source for Ge doping, Appl. Surf. Sci. 496 (2019), 143713.
[39] F. Sgarbossa, et al., Monolayer doping of germanium by phosphorus containing molecules, Nanotechnology 29 (2018).
[40] B. Long, et al., Doping top-down e-beam fabricated germanium nanowires using molecular monolayers, Mater. Sci. Semicond. Process. 62 (2017) 196–200.
[41] N. Kennedy, et al., Monolayer doping of silicon-germanium alloys: a balancing act between phosphorus incorporation and strain relaxation, J. Appl. Phys. 126 (2019).
[42] K. Cho, et al., Molecular monolayers for conformal, nanoscale doping of InP nanopillar photovoltaics, Appl. Phys. Lett. 98 (2011) 1–4.
[43] J.M. Buriak, Organometallic chemistry on silicon and germanium surfaces, Chem. Rev. 102 (2002) 1271–1308.
[44] P.W. Loscutoff, S.F. Bent, Reactivity of the germanium surface: chemical passivation and functionalization, Annu. Rev. Phys. Chem. 57 (2006) 467–495.
[45] D. Bodlaki, H. Yamamoto, D.H. Waldeck, E. Borguet, Ambient stability of chemically passivated germanium interfaces, Surf. Sci. 543 (2003) 63–74.
[46] Y. Lee, K. Park, Y.S. Cho, S. Lim, Effect of Ge surface termination on oxidation behavior, Appl. Surf. Sci. 254 (2008) 7544–7548.
[47] B. Strahlenchemie, et al., Surface oxidation states of germanium, Surf. Sci. 172 (1986) 455–465.
[48] B.E. Deal, A.S. Grove, General relationship for the thermal oxidation of silicon, J. Appl. Phys. 36 (1965) 3770–3778.
[49] Q. Xie, et al., Germanium surface passivation and atomic layer deposition of high-k dielectrics - a tutorial review on Ge-based MOS capacitors, Semicond. Sci. Technol. 27 (2012).
[50] B. William, L. Jolly, W.M. Latimer, The equilibrium Ge + GeO2 = 2 GeO. The heat of formation of germanic, J. Am. Chem. Soc. 74 (1952) 5757–5758.
[51] Y. Pauleau, J.C. Remy, Kinetics of the formation and sublimation of germanium monoxide, J. Less Common. Met. 42 (1975) 199–208.
[52] R.B. Bernstein, D. Cubicciotti, The kinetics of the reaction of germanium and oxygen, J. Am. Chem. Soc. 73 (1951) 4112–4114.
[53] F. Sgarbossa, et al., Self-limiting Sb monolayer as a diffusion source for Ge doping, Appl. Surf. Sci. 496 (2019) 8–9.
[54] S. Rivillon, Y.J. Chabal, F. Amy, A. Kahn, Hydrogen passivation of germanium (100) surface using wet chemical preparation, Appl. Phys. Lett. 87 (2005) 1–3.
[55] K. Prabhakaran, T. Ogino, Oxidation of Ge(100) and Ge(111) surfaces: an UPS and XPS study, Surf. Sci. 325 (1995) 263–271.
[56] Y. Xu, et al., Ge pMOSFETs with GeOx passivation formed by ozone and plasma post ionization, Nanoscale Res. Lett. 14 (2019).
[57] M. Green, A. Liberman, Kinetics and mechanism of oxygen adsorption on single crystals of germanium, J. Phys. Chem. Solid. 23 (1962) 1407–1415.
[58] J.T. Law, P.S. Meigs, Rates of oxidation of germanium, J. Electrochem. Soc. 104 (1957) 154.
[59] K. Park, Y. Lee, J. Lee, S. Lim, Oxidation mechanism of hydrogen-terminated Ge(1 0 0) surface, Appl. Surf. Sci. 254 (2008) 4828–4832.
[60] P. Ponath, A.B. Posadas, A.A. Demkov, Ge(001) surface cleaning methods for device integration, Appl. Phys. Rev. 4 (2017).
[61] S.R. Rivillon, et al., Wet chemical cleaning of germanium surfaces for growth of high-k dielectrics, Mater. Res. Soc. Symp. Proc. 917 (2006) 8–17.
[62] K. Choi, J.M. Buriak, Hydrogermylation of alkenes and alkynes on hydride-terminated Ge (100) surfaces, Langmuir 16 (2000) 7737–7741.
[63] C. Fleischmann, et al., Towards passivation of Ge(100) surfaces by sulfur adsorption from a (NH4)2S solution: a combined NEXAFS, STM and LEED study, J. Electrochem. Soc. 158 (2011) 589–594.
[64] C. Fleischmann, et al., Impact of ammonium sulfide solution on electronic properties and ambient stability of germanium surfaces: towards Ge-based microelectronic devices, J. Mater. Chem. C 1 (2013) 4105–4113.
[65] A.H. Boonstra, J. Van Ruler, THE ADSORPTION OF VARIOUS GASES ON CLEAN AND OXIDIZED Ge SURFACES, Surf. Sci. 4 (1966) 141–149.
[66] A.J. Van Bommel, F. Meyer, Leed measurement of H2S and II& adsorption on germanium (ill), Surf. Sci. 6 (1967) 391–394.
[67] T. Hanrath, B.A. Korgel, Chemical surface passivation of Ge nanowires, J. Am. Chem. Soc. 126 (2004) 15466–15472.
[68] S. Sun, et al., Surface termination and roughness of Ge(100) cleaned by HF and HCl solutions, Appl. Phys. Lett. 88 (2006) 1–3.
[69] Z.H. Lu, Air-stable Cl-terminated Ge(111), Appl. Phys. Lett. 520 (1996) 520–522.
[70] J. Kim, et al., Germanium surface cleaning with hydrochloric acid, ECS Trans. 3 (2019) 1191–1196.
[71] K. Park, Y. Lee, S. Lim, Modification of H-terminated Ge surface in hydrochloric acid, Appl. Surf. Sci. 254 (2008) 1842–1846.
[72] G.W. Cullen, J.A. Amick, D. Gerlich, The stabilization of germanium surfaces by ethylation, J. Electrochem. Soc. 109 (1962) 133.
[73] G. Collins, D. Aureau, J.D. Holmes, A. Etcheberry, C. O'Dwyer, Germanium oxide removal by citric acid and thiol passivation from citric acid-terminated Ge(100), Langmuir 30 (2014) 14123–14127.
[74] S.L. Heslop, A.J. Muscat, Comparison of inorganic and organic acid etching processes on germanium (100), ECS Trans. 92 (2019) 57–63.
[75] T. Alphazan, et al., Supporting Information: shallow n ++ germanium by organo-antimony monolayer doping, ACS Appl. Mater. Interfaces 9 (2017) 20179–20187.
[76] R. Duffy, M. Shayesteh, M. White, J. Kearney, M. Kelleher, Problems of N-type doped regions in germanium, their solution, and how to beat the ITRS Roadmap, ECS Trans. 35 (2011) 185–192.
[77] N.E.B. Cowern, et al., Diffusion of n-type dopants in germanium, Appl. Phys. Rev. 2 (2015).
[78] O. Hazut, et al., Parallel p-n junctions across nanowires by one-step ex situ doping, ACS Nano 8 (2014) 8357–8362.
[79] A. Tzaguy, et al., Boron monolayer doping: role of oxide capping layer, molecular fragmentation, and doping uniformity at the nanoscale, Adv. Mater. Interfac. (2020) 1–9, 1902198.
[80] P. Taheri, et al., Nanoscale Junction Formation by gas-phase monolayer doping, ACS Appl. Mater. Interfaces 9 (2017) 20648–20655.
[81] B. Long, et al., Molecular layer doping : non-destructive doping of silicon and germanium, in: Ion Implantation Technology (IIT), 2014 20th International Conference on, IEEE, 2014, https://doi.org/10.1109/IIT.2014.6939995.
[82] N. Kennedy, et al., Monolayer doping of germanium with arsenic: a new chemical route to Achieve optimal dopant activation, Langmuir 36 (2020) 9993–10002.
[83] T. Alphazan, et al., Shallow heavily-doped n++ germanium by organo-antimony monolayer doping, ACS Appl. Mater. Interfaces 9 (2017) 20179–20187.
[84] A. Satta, et al., P implantation doping of Ge: diffusion, activation, and recrystallization, J. Vac. Sci. Technol. B Microelectron. Nanom. Struct. 24 (2006) 494.
[85] J. Poate, J.W. Mayer, Laser Annealing of Semiconductors, Elsevier, 1982.
[86] K. Hemelsoet, F. Van Durme, V. Van Speybroeck, M.F. Reyniers, M. Waroquier, Bond dissociation energies of organophosphorus compounds: an assessment of contemporary ab initio procedures, J. Phys. Chem. A 114 (2010) 2864–2873.
[87] B.D. Darwent, National standard reference data series, national bureau of standards, J. Chem. Educ. 42 (1965). Washingt. DC 502.
[88] J. O'Connell, S. Biswas, R. Duffy, Chemical approaches for doping nanodevice architectures, Nanotechnology 27 (2016).
[89] G. Elliott, Oxygen as a donor element in germanium, Nature 4598 (1957) 1350–1351.
[90] R. Wittmann, S. Selberherr, A study of ion implantation into crystalline germanium, Solid State Electron. 51 (2007) 982–988.
[91] K. Benourhazi, J.P. Ponpon, Implantation of phosphorous and arsenic ions in germanium, Nucl. Instrum. Methods Phys. Res. B 71 (1992) 406–411.
[92] M. Takenaka, K. Morii, M. Sugiyama, Y. Nakano, S. Takagi, Gas phase doping of arsenic into (100), (110), and (111) germanium substrates using a metal-organic source, Jpn. J. Appl. Phys. 50 (2011).
[93] R. Milazzo, et al., N-type doping of Ge by as implantation and excimer laser annealing, J. Appl. Phys. 115 (2014).
[94] B. Long, et al., Organo-arsenic molecular layers on silicon for high-density doping, ACS Appl. Mater. Interfaces 7 (2015) 15514–15521.
[95] E. Bruno, et al., High-level incorporation of antimony in germanium by laser annealing, J. Appl. Phys. 108 (2010).
[96] C. Carraro, et al., N-type heavy doping with ultralow resistivity in Ge by Sb deposition and pulsed laser melting, Appl. Surf. Sci. 509 (2020), 145229.

[97] G. Maggioni, et al., Diffusion doping of germanium by sputtered antimony sources, Mater. Sci. Semicond. Process. 75 (2018) 118–123.

[98] S. Uppal, et al., Diffusion of boron in germanium at 800-900°C, J. Appl. Phys. 96 (2004) 1376–1380.

[99] C. Fuccio, A. La Magna, Laser Annealing Process in Semiconductor Techology, Elsevier, 2021.